

Greenhouse gases emissions from riparian wetlands: An example from the Inner Mongolia grassland region in China

Xinyu Liu^{1,2}, Xixi Lu^{1,3}, Ruihong Yu^{1,2}, Heyang Sun¹, Hao Xue¹, Zhen Qi¹, Zhengxu Cao¹, Zhuangzhuang Zhang¹, Tingxi Liu⁴

¹ Inner Mongolia Key Laboratory of River and Lake Ecology, School of Ecology and Environment, Inner Mongolia University, Hohhot 010021, China;

² Key Laboratory of Mongolian Plateau Ecology and Resource Utilization, Ministry of Education, Hohhot 010021, China;

³ Department of Geography, National University of Singapore, 117570, Singapore;

⁴ Inner Mongolia Water Resource Protection and Utilization Key Laboratory, Water Conservancy and Civil Engineering College, Inner Mongolia Agricultural University, Hohhot 010021, China

Corresponding author: Ruihong Yu (rhyu@imu.edu.cn) and Tingxi Liu (txliu@imau.edu.cn)

Abstract: Gradual riparian wetland drying is increasingly sensitive to global warming and contributes to climate change. Riparian wetlands play a significant role in regulating carbon and nitrogen cycles. In this study, we analyzed the emissions of carbon dioxide (CO₂), methane (CH₄), and nitrous oxide (N₂O) from riparian wetlands in the Xilin River Basin to understand the role of these ecosystems in greenhouse gas (GHG) emissions. Moreover, the impact of the catchment hydrology and soil property variations on GHG emissions over time and space were evaluated. Our results demonstrate that riparian wetlands emit larger amounts of CO₂ (335–2790 mg·m⁻²·h⁻¹ in the wet season and 72–387 mg·m⁻²·h⁻¹ in the dry season) than CH₄ and N₂O to the atmosphere due to high plant and soil respiration. The results also reveal clear seasonal variations and spatial patterns along the transects in the longitudinal direction. N₂O emissions showed a spatiotemporal pattern similar to that of CO₂ emissions. Near-stream sites were the only sources of CH₄ emissions, while the other sites served as sinks for these emissions. Soil moisture content and soil temperature were the essential factors controlling GHG emissions, and abundant aboveground biomass promoted the CO₂, CH₄, and N₂O emissions. Moreover, compared to different types of grasslands, riparian wetlands were the potential hotspots of GHG emissions in the Inner Mongolian region. Degradation of downstream wetlands has reduced the soil carbon pool by approximately 60%, decreased CO₂ emissions by approximately 35%, and converted the wetland

删除[Author]: and

删除[Author]: the

删除[Author]: resulted in

删除[Author]: ing

删除[Author]: reducing

删除[Author]: ing

from a CH₄ and N₂O source to a sink. Our study showed that anthropogenic activities have extensively changed the hydrological characteristics of the riparian wetlands and might accelerate carbon loss, which could further affect GHG emissions.

删除[Author]: the

Keywords: Riparian wetlands, Grasslands, Greenhouse gas, Spatial-temporal distribution, Impact factor, Xilin River Basin

删除[Author]:

1. Introduction

With the increasing rate of global warming, the change in the concentrations of greenhouse gases (GHGs) in the atmosphere is a source of concern in the scientific community (Cao et al., 2005). According to the World Meteorological Organization (WMO, 2018), the concentrations of carbon dioxide (CO₂), methane (CH₄), and nitrous oxide (N₂O) in the atmosphere have increased by 146%, 257%, and 122%, respectively, since 1750. Despite their lower atmospheric concentrations, CH₄ and N₂O absorb infrared radiation approximately 28 and 265 times more effectively at centennial timescales than CO₂ (IPCC, 2013), respectively. On a global scale, CO₂, CH₄, and N₂O together are responsible for 87% of the GHG effect (Ferrón et al., 2007).

删除[Author]: impacts

删除[Author]: contribute

删除[Author]: to

Wetlands are unique ecosystems that serve as transition zones between terrestrial and aquatic ecosystems. They play an important role in the global carbon cycle (Beger et al., 2010; Naiman and Decamps, 1997). Wetlands are sensitive to hydrological changes, particularly in the context of global climate change (Cheng and Huang, 2016). Moreover, wetland hydrology is affected by local anthropogenic activities, such as the construction of reservoirs, resulting in gradual drying. Although wetlands cover only 4–6% of the terrestrial land surface, they contain approximately 12–24% of global terrestrial soil organic carbon (SOC), thus acting as carbon sinks. Moreover, they release CO₂, CH₄, and N₂O into the atmosphere and serve as carbon sources (Lv et al., 2013). During plant photosynthesis, the amount of carbon accumulated, is generally higher than the amount of CO₂ consumed (plant respiration, animal respiration, and microbial decomposition) in the wetland; thus, the net effect of the wetland is that of a carbon sink. Wetlands are increasingly recognized as an essential part of nature, given their simultaneous functions as carbon sources and

删除[Author]: In

删除[Author]: general

删除[Author]: ion

删除[Author]: by plant's photosynthesis

删除[Author]: ption

删除[Author]: ,

删除[Author]: acted as

sinks. Excessive rainfall causes an expansion in wetland area and a sharp increase in soil moisture content, thus enhancing respiration, methanogenesis, nitrification, and denitrification rates (Mitsch et al., 2009). On the other hand, reduced precipitation or severe droughts decrease water levels, causing the wetlands to dry up. The accumulated carbon is released back into the atmosphere through oxidation. Due to the increasing impact of climate change and human activity, drying of wetlands has been widely observed in recent years (Liu et al., 2006); more than half of global wetlands have disappeared since 1900 (Mitsch and Gosselink, 2007), and this tendency is expected to continue in the future. The loss of wetlands may directly shift the soil environment from anoxic to oxic conditions, while modifying the CO₂ and CH₄ source and sink functions of wetland ecological systems (Waddington and Roulet, 2000; Zona et al., 2013).

删除[Author]: will
删除[Author]: s
删除[Author]: the
删除[Author]: contrary
删除[Author]: will result in a
删除[Author]: in
删除[Author]: will be
删除[Author]: the
删除[Author]: and modify

The Xilin River Basin in China is characterized by a marked spatial gradient in soil moisture content. It is a unique natural laboratory that may be used to explore the close relationships between the spatiotemporal variations in hydrology and riparian biogeochemistry. Wetlands around the Xilin River play an irreplaceable role with regard to local climate control, water conservation, the carbon and nitrogen cycles, and husbandry (Gou et al., 2015; Kou, 2018). Moreover, the Xilin River region is subjected to seasonal alterations in precipitation and temperature regimes. Construction of the Xilin River Reservoir has resulted in highly negative consequences, such as the drying of downstream wetlands, thereby affecting riparian hydrology and microbial activity in riparian soils. GHG emissions in riparian wetlands vary immensely. Therefore, understanding the interactions between the GHG emissions and hydrological changes in the Xilin River riparian wetlands has become increasingly important. Moreover, it is necessary to estimate the changes in GHG emissions as a result of wetland degradation at local and global scales.

删除[Author]: ,
删除[Author]: and c
删除[Author]: as well as
删除[Author]: U
删除[Author]: thus

In this work, GHG emissions from riparian wetlands and adjacent hillslope grasslands of the Xilin River Basin were investigated. GHG emissions, soil temperature, and soil moisture content were measured in the dry and wet seasons. The main objectives of this study were to (1) investigate the temporal and spatial variations in CO₂, CH₄, and N₂O emissions from the wetlands in the riparian zone, and examine the main factors affecting the GHG emissions; (2) compare the GHG emissions from the riparian wetlands with those from different types of grasslands; and (3) evaluate the impact of wetland degradation in the study area on GHG emissions.

删除[Author]: ,
删除[Author]: and
删除[Author]: ,

91

92 **2. Materials and methods**

93 **2.1 Study site**

94 The Xilin River is situated in the southeastern part of the Inner Mongolia Autonomous
95 Region in China (E115°00'–117°30', N43°26'–44°39'). It is a typical inland river of the Inner
96 Mongolia grasslands. The river basin area is 10,542 km², total length is 268.1 km, and average
97 altitude is 988.5 m. According to the meteorological data provided by the Xilinhote Meteorological
98 Station (Xi et al., 2017; Tong et al., 2004), the long-term annual mean air temperature is 1.7°C,
99 and the maximum and minimum monthly means are 20.8°C in July and –19.8°C in January,
100 respectively. The average annual precipitation was 278.9 mm for the period of 1968–2015.
101 Precipitation is distributed unevenly among the seasons, with 87.41% of the total precipitation
102 occurring between May and September.

删除[Author]: the

删除[Author]: the

删除[Author]:

103 Soil types in the Xilin River Basin are predominantly chernozems (86.4%), showing a
104 significant zonal distribution as light chestnut soil, dark chestnut soil, and chernozems from the
105 northwest to southeast. Soil types in this basin also present a vertical distribution with elevation.
106 Soluble chernozems and carbonate chernozems are primarily observed at altitudes above 1,350 m,
107 with a relatively fertile and deep soil layer. Dark chestnut soil, boggy soil, and dark meadow with
108 high humus content are distributed between the altitudes of 1,150 and 1,350 m. Meanwhile, light
109 chestnut soil, saline meadow soil, and meadow solonchak with low soil humus, a thin soil layer,
110 and coarse soil texture are distributed between the altitudes of 902 and 1,150 m (Xi et al., 2017).

删除[Author]: The chernozems are primarily

删除[Author]: s

删除[Author]: ,

删除[Author]: distributed

删除[Author]: L

111 **2.2 Field measurements and laboratory analyses**

112 In this study, five representative transects were selected as the primary measurement sites in
113 the entire Xilin River. Each transect cuts through the riparian wetlands near the river and the
114 hillslope grasslands further away (Fig. 1).

删除[Author]: from it

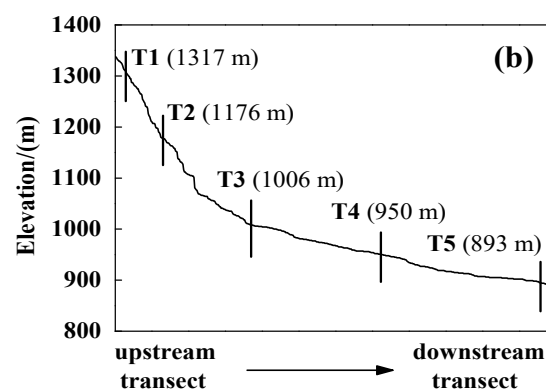
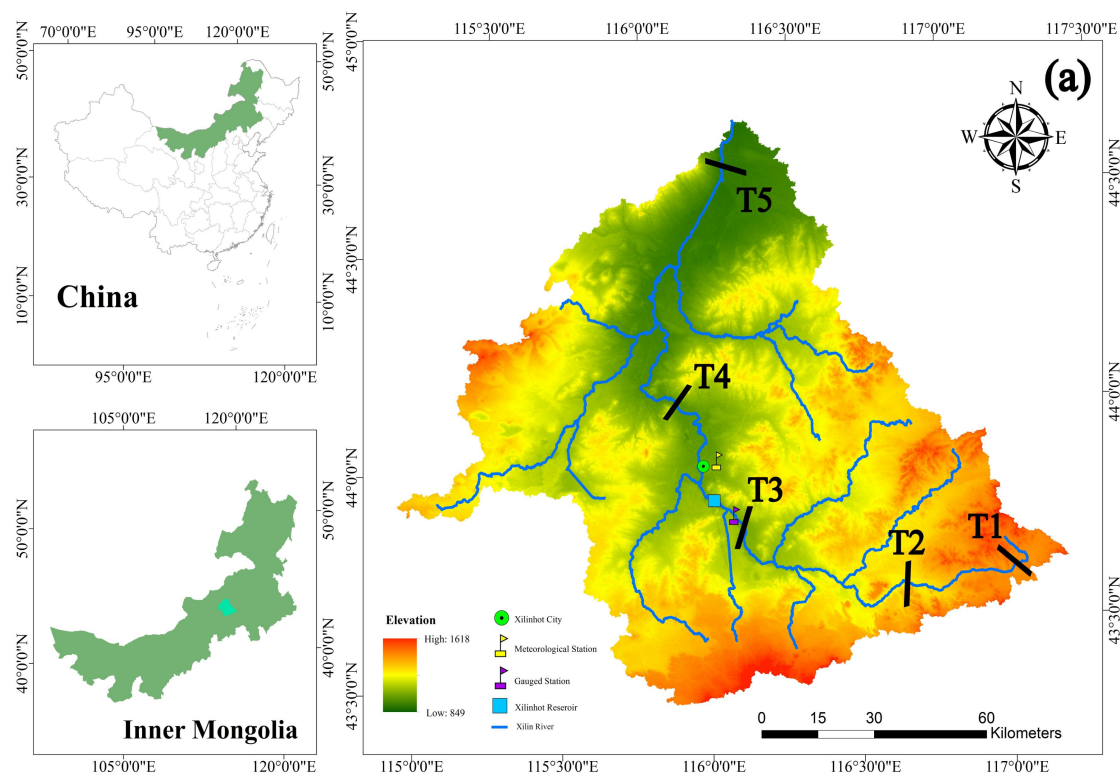


Fig. 1 (a) Location of the Xilin River Basin and distribution of five riparian-hillslope transects (T1–T5). (b) Elevation details of each transect in the Xilin River Basin.

The layout of the sampling points of each transect is shown in Fig. 2. Each sampling point, from T1–T5, was extended from either side of the river to the grassland on the slopes by using 5–7 sampling points for each transect, resulting in 24 points in total. The sampling sites on the left and right banks were defined as L1–L3 and R1–R4 from the riparian wetlands to the hillslope grasslands. As transect T3 was located on a much wider flood plain, none of its sampling points were located on the hillslope grassland. The last transect (T5) was located downstream in the dry lake and contained seven sampling points. They were defined as S1–S7, where S1, S2, and S7

删除[Author]: both sides, to

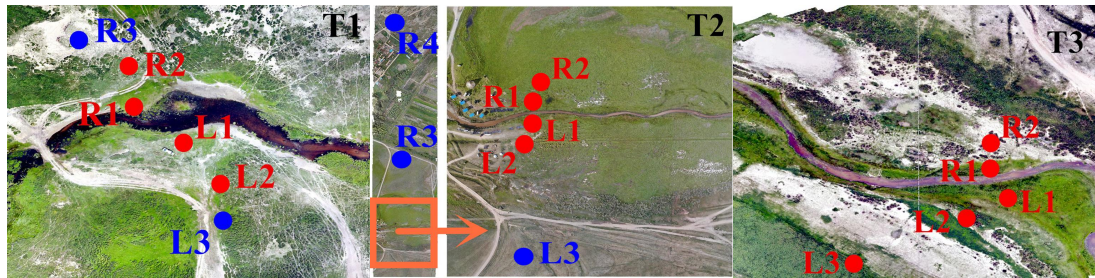
删除[Author]: ,

删除[Author]: and

were located along the lake shore (the lakeside zone), and S3–S6 were located in the dry lake bed (S3 and S4 in the mudbank, S5 in saline–alkali soil, and S6 in sand–gravel geology). Moreover, characterizations for the T1, T2, and T3 transects were located along the continuous river flow, and the T4 and T5 transects were located along the intermittent river flow.

The CO₂, CH₄, and N₂O emissions from each site were measured in August (wet season) and October (dry season) in 2018 using a static dark chamber and the gas chromatography method. The static chambers were made of a cube-shaped polyvinyl chloride (PVC) pipe (dimensions: 0.4 m × 0.2 m × 0.2 m). A battery-driven fan was installed horizontally inside the top wall of the chamber to ensure proper air mixing during measurements. To minimize heating from solar radiation, white adiabatic aluminum foil was used to cover the entire aboveground portion of the chamber. During measurements, the chambers were driven into the soil to ensure airtightness and connected with a differential gas analyzer (Li-7000 CO₂/H₂O analyzer, LI-COR, USA) to measure the changes in the soil CO₂ concentration. The air in the chamber was sampled using a 60 mL syringe at 0, 7, 14, 21, and 28 min. The gas samples were stored in a reservoir bag and taken to the laboratory for CH₄ and N₂O measurements using gas chromatography (GC-2030, Japan). The measurements were scheduled for 9:00–11:00 a.m. or 3:00–5:00 p.m.

Soil temperature (ST) was measured at depths of 0–10 cm and 10–20 cm with a geothermometer (DTM-461, Hengshui, China). Plant samples were collected in a static chamber and oven-dried in the laboratory to obtain aboveground biomass (BIO). A 100 cm³ ring cutter was used to collect surface soil samples at each site, which were placed in aluminum boxes and immediately brought back to the laboratory to measure soil mass moisture content (SMC) and soil bulk density (ρ_b) using national standard methods (NATESC, 2006). Topsoil samples were collected, sealed in plastic bags, and brought back to the laboratory to measure soil pH, electrical conductivity (EC), total soil organic carbon (TOC) content, and soil C:N ratio.



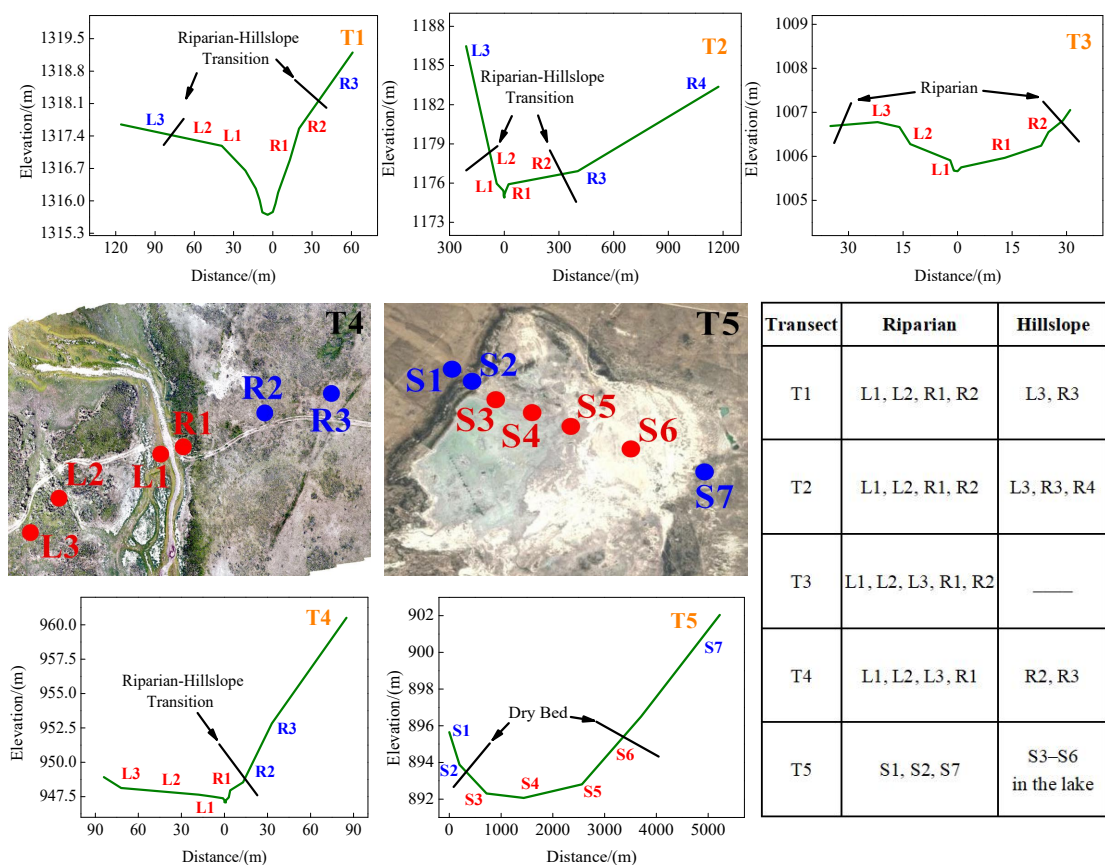


Fig. 2 Distributions of sampling points in transects T1–T5 (The images are authors' own)

Table 1. Physical and chemical properties (Mean \pm SD) of soils at various sites within each

transect

Trans ect	Sampl										
	Zone	e numb er	TOC								
			SMC10-V	SMC20-V	Soil C:N	(g·kg ⁻¹)	BIO (g)	ρ _b	pH	EC (μs/cm)	SSM (%)
T1	Riparian	12	12.16 ±	12.88 ±	12.46 ±	30.16 ±	14.67 ±	1.28 ±	7.25 ±	154.71 ±	47.77 ±
			7.55	12.05	0.91	6.54	5.44	0.07	0.62	23.70	7.04
	Hillslope	6	2.72 ± 0.91	5.05 ± 3.09	11.41 ±	10.77 ±	6.70 ± 1.48	1.45 ±	7.22 ±	82.02 ± 16.37	31.02 ±
					0.09	4.72			0.03		0.40
T2	Riparian	12	26.75 ±	12.19 ±	11.70 ±	19.96 ±	24.76 ±	1.23 ±	8.95 ±	303.88 ±	51.21 ±
			19.52	7.82	1.14	5.71	9.65	0.05	0.45	102.16	6.49
	Hillslope	9	5.85 ± 4.82	3.03 ± 1.43	9.77 ±	14.87 ±	6.10 ± 3.19	1.38 ±	8.10 ±	162.97 ±	35.09 ±
					0.88	11.21			0.13	0.55	128.18
T3	Riparian	12	28.04 ±	14.53 ±	15.80 ±	22.40 ±	6.37 ± 2.95	1.35±	9.50 ±	1233.20 ±	47.56 ±
			22.95	8.98	4.16	9.69			0.19	0.67	829.83
	L3	3	116.37 ±	113.36 ±	16.8±	36.1 ±	107.75	0.592 ±	8.5 ±	403 ± 57.21	>100

删除[Author]: s

			56.91	23.17	0.58	1.84	±16.94	0.02	0.17		
					12.52 ±	9.96 ±	11.97 ±	1.30 ±	8.84 ±	461.72 ±	44.08 ±
					2.06	1.25	4.50	0.08	0.22	314.27	7.07
T4	Riparian	12	5.42 ± 3.34	4.07 ± 4.31							
					9.97 ±	9.65 ±	7.84 ± 2.48	1.30 ±	8.23 ±	118.5 ± 8.25	39.43 ±
	Hillslope	6	3.35 ± 2.06	4.27 ± 1.94	0.50	1.05		0.09	0.14		5.55
	Dry lake	12	17.47 ±	14.49 ±	63.74 ±	31.41 ±	5.48 ± 2.35	1.16 ±	9.88 ±	7320.87 ±	58.47 ±
	bed		15.08	13.28	12.93	6.55		0.10	0.18	4300.03	7.16
T5	Lake	9	2.64 ± 1.48	2.82 ± 1.27	15.92 ±	6.35 ±	0	1.33 ±	9.41 ±	281.82 ±	37.52 ±
	shore				4.71	1.16		0.09	0.7	162.73	5.34

Note: SMC10-V - soil volumetric moisture content in 0-10 cm; SMC20-V - soil volumetric moisture content in 10-20 cm; Soil C:N - soil carbon-nitrogen ratio; TOC - total soil organic carbon; BIO - aboveground biomass; ρ_b - soil bulk density; pH - soil pH; EC - soil electrical conductivity; SSM - saturated soil moisture.

Table 2. Soil particle composition of soils at various sites within each transect

<u>Soil</u> particle composition				
Transect	Zone	Clay % (<0.002 mm)	Silt % (0.02~0.002 mm)	Sand (2.0 ~0.02 mm)
T1	Riparian	2.5	2.7	94.8
	Hillslope	9.6	6.1	85.3
T2	Riparian	5.5	5.8	90.7
	Hillslope	10.8	8.6	80.6
T3	Riparian	4.1	1.1	94.8
T4	Riparian	11.4	1.5	87.1
	Hillslope	12.7	5.9	81.4
T5	Lake shore	5.1	2.1	92.8
	Dry lake bed	46.1	4.8	49.1

2.3 Calculation of GHG emissions

The CO₂, CH₄, and N₂O emissions were calculated using Eq. 1 (Qin et al., 2016):

$$F = \frac{V}{A} \times \frac{dc}{dt} \times \rho = H \times \frac{dc}{dt} \times \frac{M}{V} \times \left(\frac{273.15}{273.15 + t} \right) \tag{1}$$

Where F denotes the flux of CO₂, CH₄, and N₂O emissions (mg·m⁻²·h⁻¹), H is the height of the static chamber (0.18 m), M is the relative molecular weight (44 for CO₂ and N₂O, and 16 for CH₄), V is the volume of gas in the standard state (22.4 L·mol⁻¹), dc/dt is the rate of change of the gas concentration (10⁻⁶·h⁻¹), and T is the temperature in the black chamber (°C).

The annual cumulative emissions were calculated using Eq. 2 (Whiting G and Chanton J., 2001):

$$M = \sum \frac{F_{i+1} + F_i}{2} \times (t_{i+1} - t_i) \times 24 \quad (2)$$

Where M denotes the total cumulative emission amounts of CO₂, CH₄, or N₂O (kg·hm²), *F* is the emission flux of CO₂, CH₄, or N₂O, *i* is the sampling frequency, and *t_{i+1}-t_i* represents the interval between two adjacent measurement dates.

In this study, a 100-year scale was selected to calculate the global warming potential (GWP) of soil CH₄ and N₂O emissions (Whiting G and Chanton J., 2001):

$$GWP = 1 \times [CO_2] + 25 \times [CH_4] + 298 \times [N_2O] \quad (3)$$

Where 25 and 298 are the GWP multiples of CH₄ and N₂O relative to CO₂ on a 100-year time scale, respectively.

2.4 Statistical Analysis

All statistical analyses were performed using SPSS for Windows version 18.0 (SPSS Inc., Chicago, IL, USA). Statistical significance was set at *P* < 0.05. Pearson correlation analysis was conducted to estimate the relationships between GHG_v fluxes and environmental variables. A Wilcoxon test was used to determine the differences s in the GHG_v fluxes between the two seasons.

3. Results

3.1 Spatiotemporal patterns of SMC for each transect

The temporal and spatial variations in SMC10 occurred in the following order: wet season > dry season and riparian wetlands > hillslope grasslands (Fig. 3a, c, e). Similar variations were observed in SMC20 (Fig. 3b, d, f). The average SMC10 and SMC20 in the continuous river transects in the riparian zones (SMC10 values were 37.44% in the wet season and 19.40% in the dry season, while, SMC20 values were 25.96% in the wet season and 17.39% in the dry season) were higher than those in the hillslope grasslands (SMC10 values were 9.12% in the wet season and 4.15% in the dry season; SMC20 values were 6.51% in the wet season and 5.96% in the dry season). During the study period, both SMC10 and SMC20 changed as the distance from the river increased, and the highest value was observed at the near-stream sites (L1 and R1). SMC10 fluctuations were low in the intermittent transect compared with those in the upstream transects,

删除[Author]:

删除[Author]: s

删除[Author]: of

删除[Author]: s

删除[Author]: in

删除[Author]:

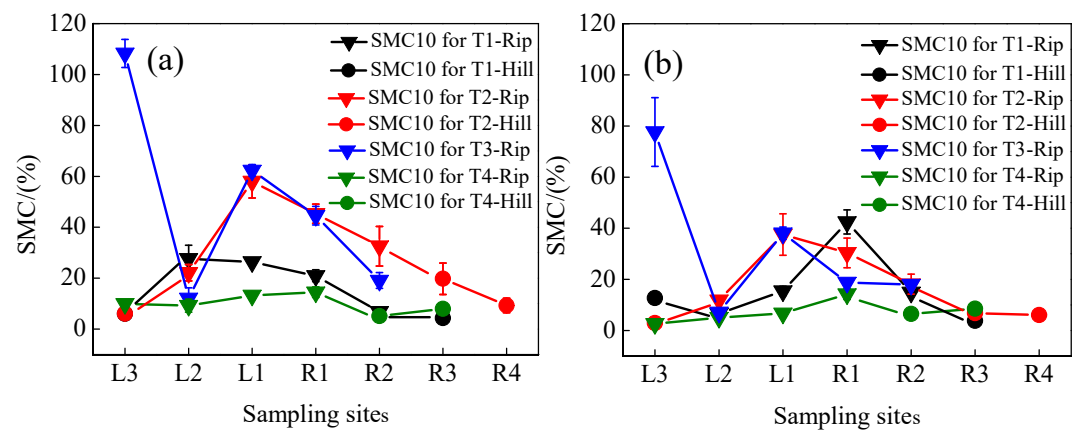
删除[Author]: ;

删除[Author]: to

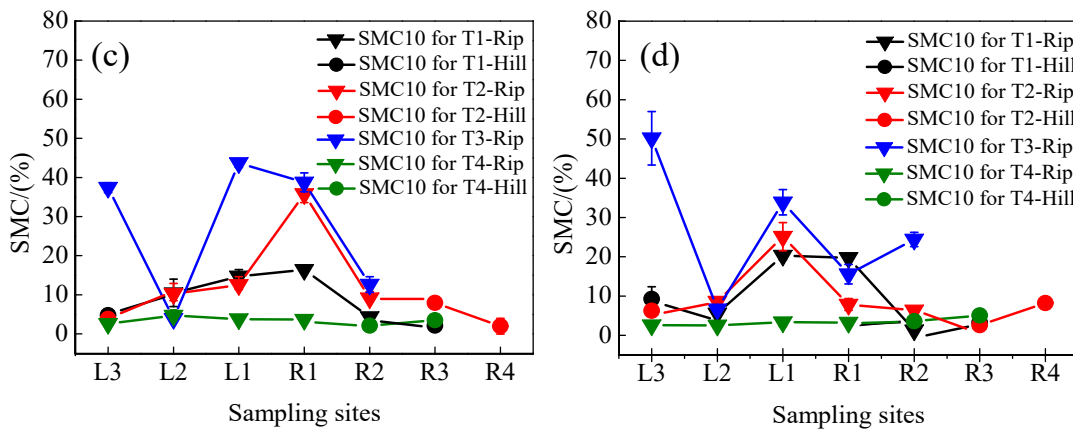
with mean values being 11.79% in the wet season and 3.72% in the dry season in the riparian areas. The mean SMC10 in the hillslopes was 6.58% in the wet season and 2.86% in the dry season. SMC20 showed similar fluctuation; it was 7.22% in the wet season and 2.98% in the dry season in the riparian areas, and 7.56% in the wet season and 4.4% in the dry season in the hillslopes. In transect T5, average SMC10 and SMC20 at the center of the lake (SMC10 values were 29.00% in the wet season and 13.36% in the dry season; SMC20 values were 29.30% in the wet season and 9.69% in the dry season) were higher than those along the lake shore (SMC10 values were 4.90% in the wet season and 3.13% in the dry season; SMC20 values were 3.34% in the wet season and 5.22% in the dry season).

删除[Author]: a
删除[Author]: of
删除[Author]: ,

Wet season



Dry season



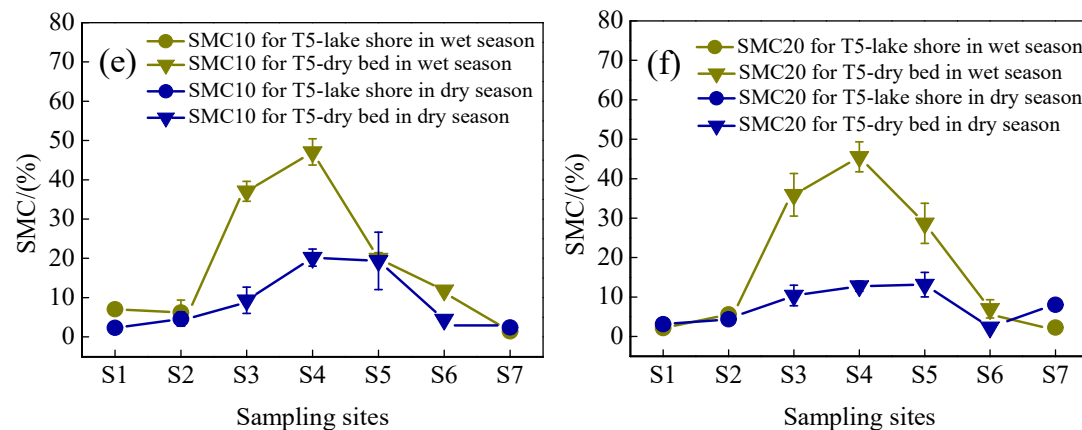
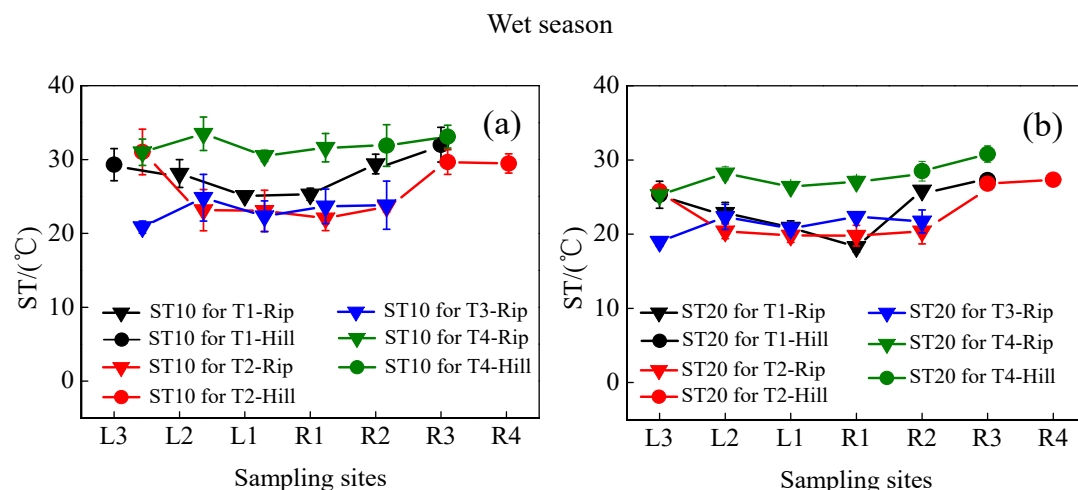


Fig. 3 Soil mass moisture contents (SMCs) at soil depths of 0–10 cm (SMC10) and 10–20 cm (SMC20) for transects T1–T5 in the wet and dry seasons. Error bars represent the SD about the mean.

3.2 Spatiotemporal patterns of ST in each transect

Spatiotemporal differences in ST during the entire observation period are displayed in Fig. 4.

ST variations in the wet season (mean 27.4°C) were noticeably higher than those in the dry season (mean 8.97°C). Moreover, ST at riparian sites (mean 26.0°C in the wet season and 8.41°C in the dry season) was slightly lower than that at the hillslope grasslands (mean 30.9°C in the wet season and 10.3°C in the dry season) for the 0–10 cm soil depth, with the exception of transect T5. Similar results were observed for the 10–20 cm soil depth.



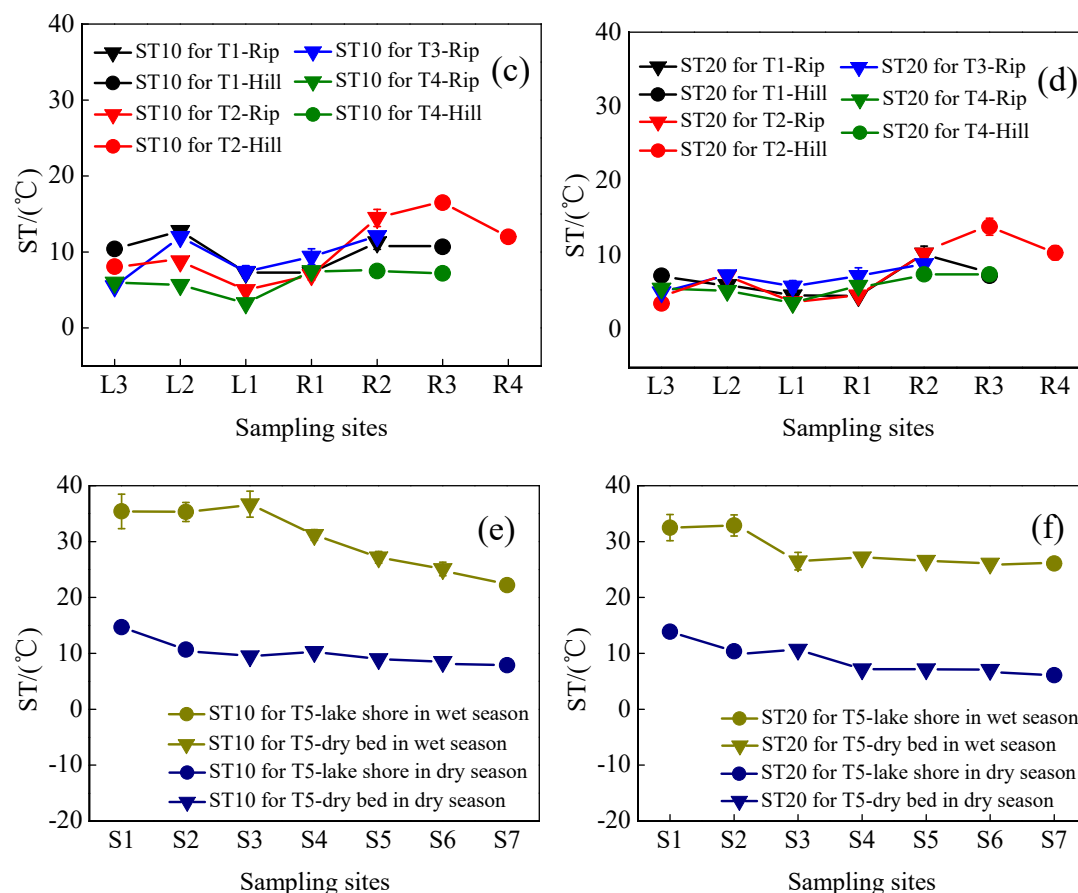


Fig. 4 Soil temperatures (STs) at soil depths of 0–10 cm (ST10) and 10–20 cm (ST20) for transects T1–T5 in the wet and dry seasons. Error bars represent the SD about the mean.

3.3 Spatiotemporal patterns of GHG emissions in each transect

Figure 5 shows the spatiotemporal variations in GHG emissions in the wet and dry seasons in each transect. CO₂ emissions in each transect were higher in the wet season than in the dry season. The average emissions in the riparian wetland transects T1–T4 ($1582.09 \pm 679.34 \text{ mg} \cdot \text{m}^{-2} \cdot \text{h}^{-1}$ in the wet season and $163.24 \pm 84.98 \text{ mg} \cdot \text{m}^{-2} \cdot \text{h}^{-1}$ in the dry season) were higher than the transects in the hillslope grasslands ($1071.54 \pm 225.39 \text{ mg} \cdot \text{m}^{-2} \cdot \text{h}^{-1}$ in the wet season and $77.68 \pm 25.32 \text{ mg} \cdot \text{m}^{-2} \cdot \text{h}^{-1}$ in the dry season). High CO₂ fluxes occurred in the riparian zones, while lower CO₂ fluxes were observed in the hillslope grasslands in continuous river transects (T1, T2, and T3). Transect T4 exhibited lower CO₂ emission in the riparian wetlands near the channel than at sites away from the channel. CO₂ emissions in transect T5 in the wet and dry seasons decreased from the lake shore to the lake center.

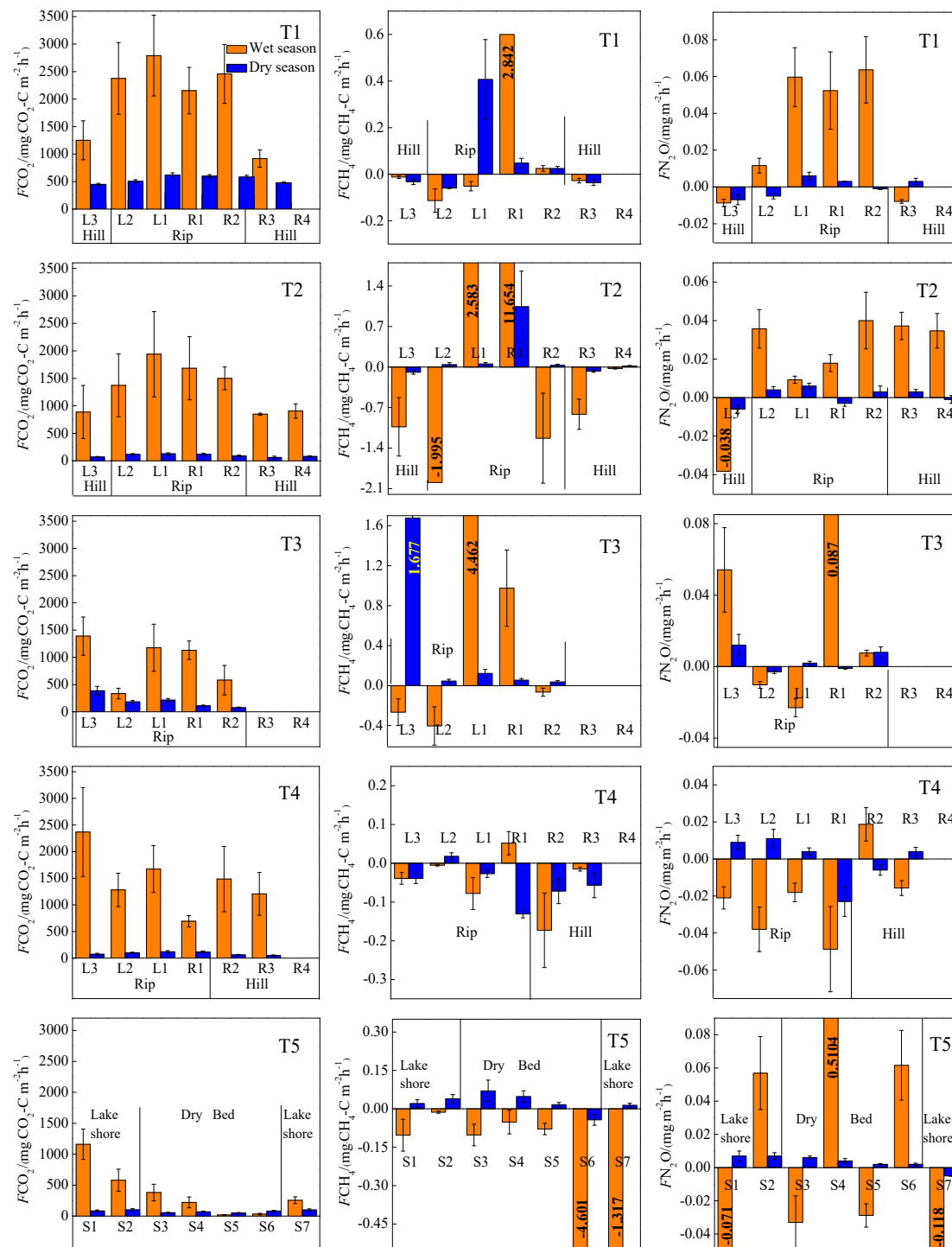


Fig. 5 Spatiotemporal patterns of CO₂ (first column), CH₄ (second column), and N₂O (third column) emission (F) for each transect. Data are shown for the wet season (orange) and the dry season (blue). Error bars depict standard deviation.

CH₄ emissions at the continuous river flow transects (T1, T2, and T3) varied between the wet and dry seasons, except for those at T4 (characterized by intermittent river flow) and T5 (the dry

删除[Author]: s
删除[Author]: and
删除[Author]: error
删除[Author]: are the
删除[Author]: s
删除[Author]: transects with
删除[Author]: season

lake). In ~~the~~ wet season, the near-stream sites (L1 and R1) in T1, T2, and T3 were characterized as high CH₄ sources (average ~~3.74 ± 3.81~~ mg·m⁻²·h⁻¹), but the sites located away from the river gradually turned into CH₄ sinks. Moreover, all the sites in transects T4 and T5 were sinks. CH₄ emissions (mean value: 0.2 ± 0.45 mg·m⁻²·h⁻¹) at the wetland sites were always lower in ~~the~~ dry season than those in ~~the~~ wet season. However, the sites on the hillslope grasslands served as CH₄ sinks (mean ~~value~~: -0.05 ± 0.03 mg·m⁻²·h⁻¹). In transect T5, CH₄ emissions ~~showed~~ the opposite trend; a CH₄ sink was observed in ~~the~~ wet season, but it was transformed into a CH₄ source in ~~the~~ dry season.

Similar to the CO₂ and CH₄ emissions, N₂O emissions showed a distinct spatiotemporal pattern ~~in~~ all the transects. N₂O emissions in ~~the~~ wet season were higher than those in ~~the~~ dry season. These emissions were higher in ~~the~~ riparian wetlands than in ~~the~~ hillslope grasslands. Moreover, almost all ~~sites with continuous river flow~~ were N₂O sources, while more than half of the sites with intermittent river flow were sinks.

Table 3 shows that CO₂ fluxes were significantly correlated between the wet ~~and dry seasons~~, while CH₄ and N₂O fluxes were not correlated ~~between the~~ two seasons.

Table 3 Significant correlations between GHGs fluxes and two seasons (n=31)

GHG flux	FCO ₂ in the wet season - FCO ₂ in	FCH ₄ in the wet season - FCH ₄ in	FN ₂ O in the wet season - FN ₂ O in
	the dry season	the dry season	the dry season
Significant			
correlations (P)	0.000	0.133	0.290

Note: P < 0.05 denotes ~~s~~ significant correlation, and P > 0.05 denotes ~~s~~ no significant correlation.

3.4 Spatiotemporal patterns of GHG emission ~~in upstream and downstream~~ areas

Figure 6 shows the detailed spatial and seasonal ~~patterns~~ of GHG emission ~~in the wet and dry~~ seasons in the longitudinal direction from the upstream (T1, T2, and T3) to the downstream areas (T4 and T5). The CO₂, CH₄, and N₂O emissions were calculated ~~using~~ the average values of the respective emissions in the wetlands and hillslope grasslands in each transect.

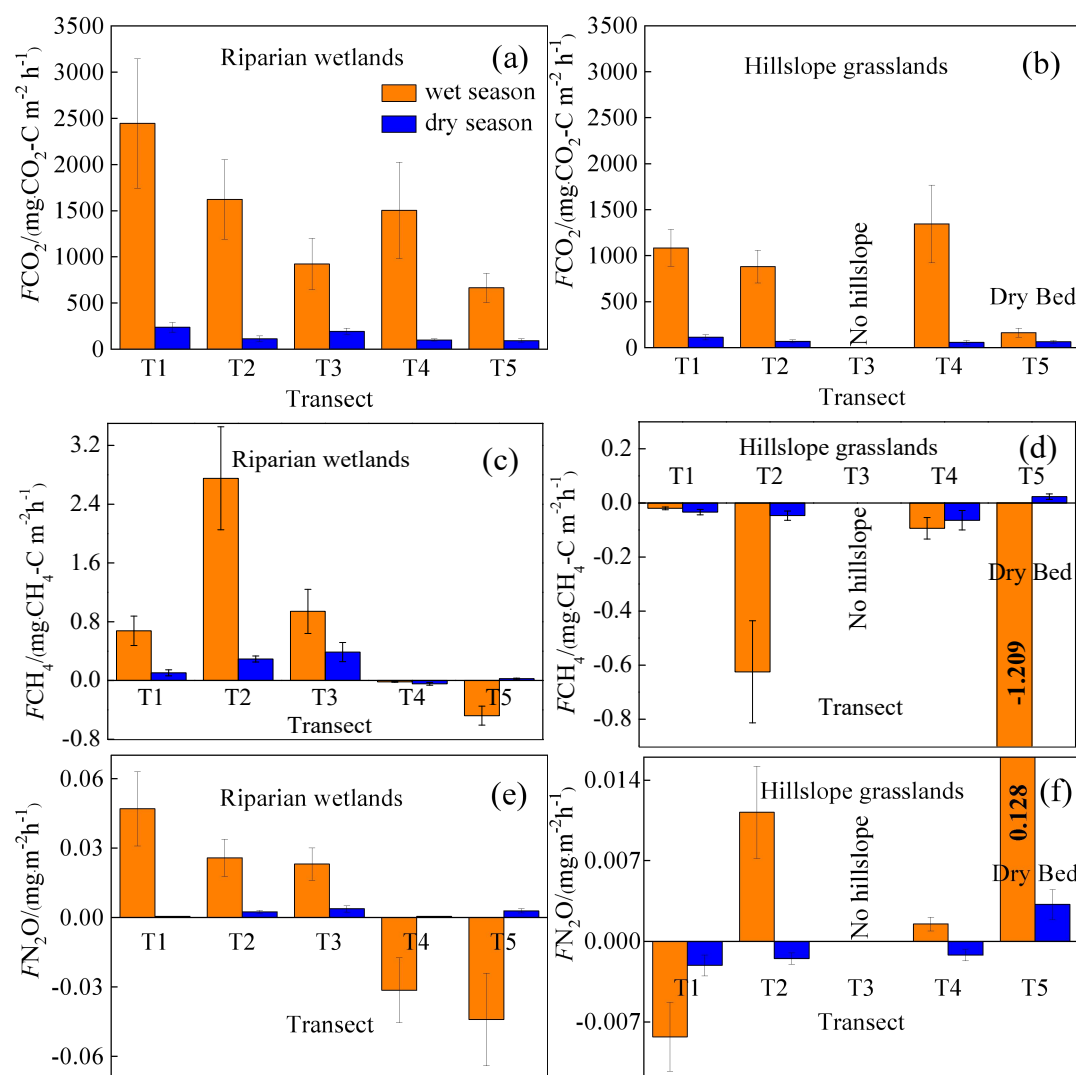


Fig. 6 Spatiotemporal patterns of CO₂ (first line), CH₄ (second line), and N₂O (third line)

emissions (F) in the upstream (T1, T2, and T3) and downstream areas (T4 and T5). Bars represent the mean values for each transect and error bars show the standard errors.

CO₂ emissions at the riparian wetlands (Fig. 6(a)) in the wet season decreased from $2,444.69 \pm 228.58 \text{ mg} \cdot \text{m}^{-2} \cdot \text{h}^{-1}$ in the upstream area to $665.08 \pm 347.57 \text{ mg} \cdot \text{m}^{-2} \cdot \text{h}^{-1}$ downstream, and the corresponding values for the dry season were $238.12 \pm 48.20 \text{ mg} \cdot \text{m}^{-2} \cdot \text{h}^{-1}$ and $94.14 \pm 7.67 \text{ mg} \cdot \text{m}^{-2} \cdot \text{h}^{-1}$, respectively. However, in the hillslope grasslands (Fig. 6(b)), CO₂ emissions exhibited no significant seasonality between the upstream and downstream areas, with mean values being $1,103.40 \pm 190.44 \text{ mg} \cdot \text{m}^{-2} \cdot \text{h}^{-1}$ in the wet season and $79.18 \pm 24.52 \text{ mg} \cdot \text{m}^{-2} \cdot \text{h}^{-1}$ in the dry season. In addition, the CO₂ emissions in transect T5 were lower for both months, with the averages of $162.83 \pm 149.15 \text{ mg} \cdot \text{m}^{-2} \cdot \text{h}^{-1}$ and $63.26 \pm 12.40 \text{ mg} \cdot \text{m}^{-2} \cdot \text{h}^{-1}$ in the wet and dry season,

299 respectively. The upstream riparian zones exhibited higher CO₂ emissions (894.32 ± 868.47
300 mg·m⁻²·h⁻¹) than their downstream counterparts (621.14 ± 704.10 mg·m⁻²·h⁻¹). Mean CO₂
301 emissions showed no significant differences in the grasslands, averaging 524.16 ± 450.10
302 mg·m⁻²·h⁻¹ upstream and 508.06 ± 534.77 mg·m⁻²·h⁻¹ downstream.

303 CH₄ emissions showed a marked spatial pattern in the riparian zones from upstream to
304 downstream (Fig. 6(c)). The transects with continuous river flow were CH₄ sources in the wet and
305 dry seasons, with average emissions of 1.42 ± 3.41 mg·m⁻²·h⁻¹ and 0.27 ± 0.49 mg·m⁻²·h⁻¹,
306 respectively, while those with intermittent river flow served as CH₄ sinks, with the corresponding
307 means of -0.21 ± 0.45 mg·m⁻²·h⁻¹ and -0.02 ± 0.05 mg·m⁻²·h⁻¹, respectively. Moreover, the
308 hillslope grassland sites in all transects were CH₄ sinks (Fig. 6(d)).

309 N₂O emissions in riparian wetlands (Fig. 7(e)) showed spatial patterns similar to those of
310 CH₄ emissions. In the wet season, the transects with continuous river flow served as N₂O sources,
311 with a mean emission of 0.031 ± 0.031 mg·m⁻²·h⁻¹, meanwhile, transects with intermittent river
312 flow acted as N₂O sinks with an average emission of -0.037 ± 0.05 mg·m⁻²·h⁻¹. In the dry season,
313 N₂O emissions occurred as weak sources in the longitudinal transects, exhibiting an average
314 emission of 0.002 ± 0.007 mg·m⁻²·h⁻¹. However, the N₂O emission in the hillslope grasslands did
315 not show any spatial patterns (Fig. 7(f)).

316 4. Discussion

317 4.1 Main factors influencing GHG emissions

318 4.1.1 Effects of SMC on GHG emissions

319 SMC constitutes one of the main factors affecting GHG emission in wetlands. In this study,
320 transects T1–T4 were characterized by a marked spatial SMC gradient (i.e., a gradual decrease in
321 SMC10 and SMC20 from the riparian wetlands to the hillslope grasslands and from the upstream
322 to downstream regions (Fig. 3)). The CO₂, CH₄, and N₂O emissions showed a similar trend. Table
323 4 shows that SMC10 is positive correlated with CO₂ emission (P < 0.05), and that SMC10 and
324 SMC20 are significantly positively correlated with CH₄ emission (P < 0.01), and with N₂O
325 emission (P < 0.05 and P < 0.01, respectively). These results indicate the influence of wetland
326 SMC on GHG emission.

327 Typically, the optimal SMC associated with CO₂ emission in the riparian wetlands ranges
328 from 40 to 60% (Sjögersten et al., 2006), creating better soil aeration, and improving soil

删除[Author]: However, m

删除[Author]: season

删除[Author]: the

删除[Author]: s

删除[Author]: ,

删除[Author]: value

删除[Author]: the

删除[Author]: value

删除[Author]: ,

删除[Author]: those

删除[Author]: were

删除[Author]: value

删除[Author]: ing

删除[Author]: s

删除[Author]: d

删除[Author]: s

删除[Author]: include

删除[Author]: In

删除[Author]: ,

删除[Author]: s

设置格式[Author]: 字体: 非倾斜

删除[Author]: s

设置格式[Author]: 字体: 非倾斜

删除[Author]: ,

删除[Author]: SMC10 and SMC20 are highly positive

删除[Author]: s

设置格式[Author]: 字体: 非倾斜

设置格式[Author]: 字体: 非倾斜

删除[Author]: d

删除[Author]: s

删除[Author]:

删除[Author]: values

删除[Author]: s

microorganism activity and respiration in plant roots, thereby promoting CO₂ emission. Excessive SMC reduces soil gas transfer due to the formation of an anaerobic environment in the soil, and microbial activity is lowered, favoring the accumulation of organic matter (Hui., 2014). The SMC of the hillslope grasslands was found to be less than 10%. Low soil moisture inhibits the growth of vegetation, with few vegetation residues and litters. Meanwhile, low soil moisture is not conducive to the survival of soil microorganisms, leading to lower CO₂ emission from the hillslope grasslands than from the riparian zones (Moldrup et al., 2000; Hui., 2014). Similar results were obtained in our study. The change in CO₂ emission in transect T5 was contrary to the changes in SMC10 and SMC20, likely because the optimal range of soil C:N is between 10-12 (Pierzynski et al., 1994), but the value in the dry lake bed of T5 is higher than 60. The high soil C:N resulted in nitrogen limitation in the process of decomposition of organic matter by microorganisms. Further, other sediment properties (like Soil pH > 9.5) for this transect were not conducive to the survival of microorganisms (Table 1), and the increase in SMC did not increase the respiration activity of the microorganisms.

The highest CH₄ emissions were observed at the near-stream sites (i.e., L1 and R1) in T1, T2, and T3, with average SMC of 30.29%, while the SMC at the other sites, which were either weak sources or sinks, averaged at 14.57%. These results indicate that a higher SMC is favorable for CH₄ emissions. This may be because a higher SMC accompanies soil in a reduced state, which is beneficial for CH₄ production and inhibits CH₄ oxidation. A similar result was reported by Xu et al. (2008). They conducted experiments analyzing CH₄ emissions from a variety of paddy soils in China, and showed that CH₄ production rates increased with the increase in SMC at the same incubation temperature. Meng et al. (2001) also reported that water depth was the main factor affecting CH₄ emissions from wetlands. When the water level dropped below the soil surface, the decomposition of organic matter accelerated, and CH₄ emission decreased. If the oxide layer is large, the soil is transformed into a CH₄ sink (Meng et al., 2011).

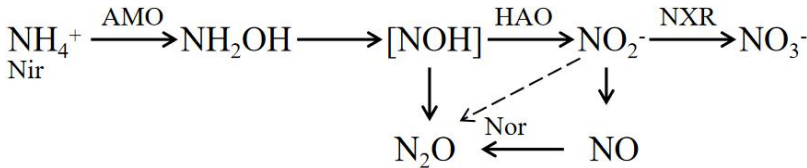
The N₂O fluxes showed a clear spatial pattern associated with the changes in SMC. The moisture content of wetland soils directly affects the aeration status of the soil. Besides, the aeration status affects the partial pressure of oxygen, which has an important impact on nitrifying/denitrifying bacterial activity and ultimately affects soil N₂O emissions (Zhang et al., 2005). Table 4 shows that N₂O emission is significantly positively correlated with SMC10 and

删除[Author]: s'
删除[Author]: the
删除[Author]: of
删除[Author]: s,
删除[Author]: whereas e
删除[Author]: On the contrary, t
删除[Author]: is
删除[Author]: a decrease in
删除[Author]: s
删除[Author]: to those in
删除[Author]: s
删除[Author]: s
删除[Author]: were
删除[Author]: the
删除[Author]: ,
删除[Author]: ly
删除[Author]: largest
删除[Author]: the
删除[Author]: values
删除[Author]: denotes
删除[Author]: a
删除[Author]: of
删除[Author]: s
删除[Author]: 's
删除[Author]: s are

SMC20 ($P < 0.01$). Generally, when SMC is below the saturated water content, the microorganisms are in an aerobic environment, and N_2O mainly comes from the nitrification reaction. N_2O emission increases with increase in SMC (Niu et al., 2017; Yu et al., 2006). In our study, the sampling sites with higher SMC (riparian zones and some hillslope grassland zones in the upstream transects) have higher N_2O emissions. When SMC increases to the saturated water content or is in a flooded state, the system is an anaerobic environment, and the nitrous oxide reductase activity is higher due to excessively high SMC, which is conducive to denitrification and eventually produces N_2 (Niu et al., 2017; Yu et al., 2006), such as at site L1 in transect T3 in this study. Ulrike et al. (2004) showed that denitrification was the main process under flooded soil conditions in wetland soils, and that the release of N_2 exceeds that of N_2O . These findings are consistent with those of Liu et al. (2003), who showed that SMC is an essential factor affecting N_2O emission.

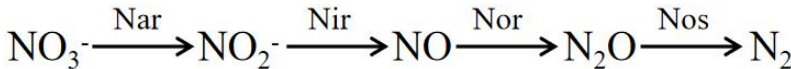
371

372 Nitrification:



373

374 Denitrification:



375

376 The enzymes involved in the formula include Ammonia monooxygenase (AMO),
377 Hydroxylamine oxidase (HAO), Nitrite REDOX enzyme (HAO), nitrate reductase (Nar), nitrite
378 reductase (Nir), Nitric oxide reductase (Nor), and Nitrous oxide reductase (Nos).

379 4.1.2 Effects of ST on GHG emissions

380 ST was another important factor affecting CO_2 emission in this study; it was found to be
381 significantly correlated with CO_2 emission ($P < 0.01$) (Table 4). The activity of soil
382 microorganisms increases with rising soil temperature, leading to increased respiration, and
383 consequently higher CO_2 emission (Heilman et al., 1999). Previous studies have reported that ST
384 partially controls seasonal CO_2 emission patterns (Inubushi et al., 2003). Concurrently, CO_2
385 emissions in the wet season were significantly higher than those in the dry season in this study.

386 CH_4 emissions showed a clear seasonal pattern, likely because high summer temperatures

删除[Author]: was

删除[Author]: were

删除[Author]: came

删除[Author]: s

删除[Author]: the

删除[Author]: of

删除[Author]: was

删除[Author]: Nos

删除[Author]: was

删除[Author]: was

删除[Author]: d

删除[Author]: s

删除[Author]: the

删除[Author]: s

删除[Author]: ,

删除[Author]: as this parameter

删除[Author]: s

设置格式[Author]: 字体: 非倾斜

删除[Author]: s

删除[Author]: ,

删除[Author]: s

删除[Author]: Therefore

improve the activity of both CH₄-producing and -oxidizing bacteria (Ding et al., 2010). However, as Table 4 indicates, the correlation between CH₄ emission and temperature was not significant in this study, likely because SMC was a more critical factor than temperature in our study region given its very dry climate. SMC showed a positive correlation with GHG emissions. In addition, SMC affected ST to a certain extent, while the interactions between SMC and ST had a mutual influence on CH₄ emission. During the study period, the near-stream sites (L1 and R1) maintained a super-wet state on the ground surface for a long time, which was beneficial for the production of CH₄. However, the wetlands maintained a state without water accumulation on the soil surface in August, which was conducive to the oxidative absorption of CH₄. SMC thus masked the effect of ST on CH₄ emissions.

Previous studies have indicated that temperature is an important factor affecting N₂O emission (Sun et al., 2011) through primary mechanisms impacting the nitrifying and denitrifying bacteria in the soil. As Table 4 shows, the correlations between N₂O emission and ST10 and ST20 were poor ($P > 0.05$). This can be attributed to the wide suitable temperature range for nitrification-denitrification and weak sensitivity to temperature. Malhi et al. (1982) found that the optimum temperature for nitrification was 20 °C, and that it inhibits entirely at 30 °C. However, Brady (1999) believed that the suitable temperature range for nitrification is 25~35 °C, and that nitrification inhibits below 5 °C or above 50 °C. This shows that the temperature requirements of nitrifying microorganisms in wetland soils are possibly different in different temperature belts. The suitable temperature range was the performance of the long-term adaptability of nitrifying microorganisms. Meanwhile, several studies have revealed that denitrification can be carried out in a wide temperature range (5~70 °C), and that it is positively related to temperature (Fan., 1995). However, the process is inhibited when the temperature is too high or too low. The average ST in the wet season was 27.4 °C, conducive to the growth of denitrifying microorganisms, while that in dry season was 8.97 °C, and the microbial activity was generally low (Sun et al., 2011). Furthermore, ST fluctuations were low both in the wet and dry seasons. Therefore, the effect of ST on N₂O emission may have been masked by other factors, such as moisture content.

4.1.3 Effects of BIO and soil organic matter content on GHG emissions

CO₂ and CH₄ emissions were higher in the riparian wetlands than in the grasslands, mainly because of the greater vegetation cover in the former. Typically, CO₂ emissions in the riparian

删除[Author]: that
删除[Author]: s
删除[Author]: is
删除[Author]: could be
删除[Author]: with
删除[Author]: s
删除[Author]: s
删除[Author]: that
删除[Author]: s
删除[Author]: are
设置格式[Author]: 字体: 非倾斜
删除[Author]: will
删除[Author]: was
删除[Author]: ~
删除[Author]: the
删除[Author]: It
删除[Author]: ed
删除[Author]: were
删除[Author]: could
删除[Author]: ~
删除[Author]: was
删除[Author]: will be
删除[Author]: season
删除[Author]: s
删除[Author]: was
删除[Author]: from

417 wetlands originate from plants and microorganisms, with plant respiration accounting for a large
418 proportion in the growing season. Previous studies have shown that plant respiration accounts for
419 35–90% of the total respiration in the wetland ecosystem (Johnson-Randall and Foote, 2005). The
420 good soil physicochemical properties and high soil TOC content of the riparian wetlands improve
421 both the activity of soil microorganisms and plant root respiration. As Table 4 shows, BIO is
422 significantly correlated with CO₂ ($P < 0.05$) and CH₄ ($P < 0.01$) emissions. These results are
423 indicated by the significant linear positive correlation between the respiration rate and plant
424 biomass (Lu et al., 2007). Higher plant biomass storage can achieve more carbon accumulation
425 during photosynthesis and higher exudate release by the roots. This, in turn, promotes the
426 accumulation of soil organic matter. Increased amount of organic matter stimulates the growth and
427 reproduction of soil microorganisms, ultimately promoting CO₂ and CH₄ emission. Moreover,
428 plants act as gas channels for CH₄ transmission, and a larger amount of biomass promotes CH₄
429 emission, given the increased number of channels. In transect T3, the high CO₂ emission observed
430 at site L3 can be attributed to the relatively high levels of SMC, BIO, and soil nutrients, which
431 stimulate microbial respiration rates.

432 BIO had a weak correlation with N₂O emission (Table 4), which indicates that plants increase
433 N₂O production and emission, although this may not be the most critical factor. Previous studies
434 have reported mechanisms wherein the plants are able to absorb the N₂O produced in the soil
435 through the root system before releasing it into the atmosphere. Additionally, the root exudates of
436 plants can enhance the activity of nitrifying and denitrifying bacteria in the soil, ultimately
437 promoting the production of N₂O. Finally, oxygen stress caused by plant respiration can regulate
438 the production and consumption of N₂O in the soil, eventually affecting the conversion of nitrogen
439 in the soil (Koops et al., 1996; Azam et al., 2005).

440 Site L3 in transect T3 was covered by tall reeds, and its BIO was much higher than that of
441 any of the other sites; thus, the data for this site were excluded from the correlation analysis.

删除[Author]: Good
删除[Author]: total organic carbon (
删除[Author]:)
删除[Author]: that
删除[Author]: the
设置格式[Author]: 字体: 非倾斜
设置格式[Author]: 字体: 非倾斜
删除[Author]: can be attributed to
删除[Author]: s
删除[Author]: a
删除[Author]: s
删除[Author]: s
删除[Author]: the
删除[Author]: s
删除[Author]: s
删除[Author]:
删除[Author]: can
删除[Author]: those

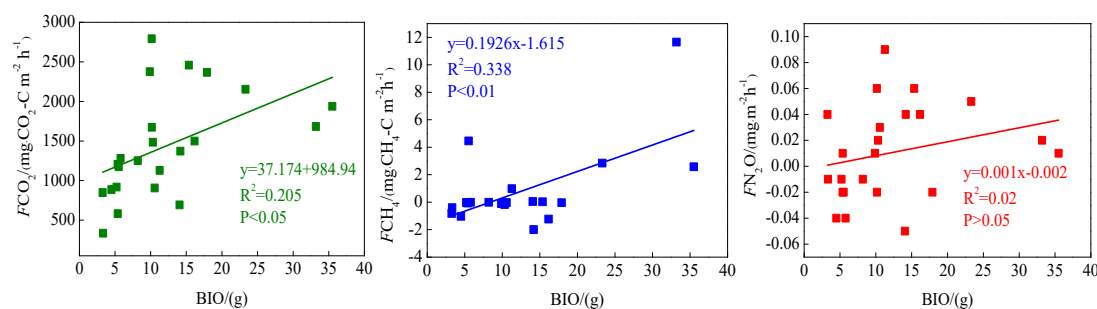


Fig. 7 Correlation between aboveground biomass (BIO) and GHG emission (F)

Soil C:N ratio refers to the ratio of the concentration biodegradable carbonaceous organic matter to nitrogenous matter in the soil, and it forms a soil matrix with TOC. TOC decomposition provides energy for microbial activity, while the C:N ratio affects the decomposition of organic matter by soil microorganisms (Gholz et al., 2010). The correlation results (Fig. 8) indicate that TOC had a weak positive correlation with CO₂ emission ($P > 0.05$), but the soil C:N ratio had a significant negative correlation with CO₂ emission ($P < 0.05$), indicating that nitrogen has a limiting effect on soil respiration by affecting microbial metabolism. Liu et al. (2019) have reported that N addition promotes CO₂ emission from wetlands soil, and the effect of organic N input was significantly higher than that of inorganic N input. Organic carbon acts as a carbon source for the growth of plants and microorganisms, which boosts their respiration. Moreover, TOC has a significant correlation with N₂O emissions ($P < 0.05$). Most heterotrophic microorganisms use soil organic matter as carbon and electron donors (Morley N and Baggs E M., 2010). Soil carbon sources have an important influence on microbial activity. Nitrifying or denitrifying microorganisms need organic matter to act as the carbon source during the assimilation of NH₃ or NO₃⁻. High content of organic matter in the soil can promote the concentration of heterotrophic nitrifying bacteria, consume dissolved oxygen in the medium, and cause the soil to become more anaerobic, thereby slowing down autotrophic growth nitrifying bacteria. This reduces the nitrification rate, ultimately promoting N₂O release. Enwall et al. (2005) studied the effect of long-term fertilization on soil denitrification microbial action intensity. They found that the soil with long-term organic fertilizer application has a significant increase in organic matter content, and consequently, a significant increase in denitrification activity. Typically, low soil C:N ratios are favorable for the decomposition of microorganisms, the most

删除[Author]: s

删除[Author]: and

删除[Author]: the

删除[Author]: s

删除[Author]: s

删除[Author]: s

删除[Author]: s

删除[Author]: reported that

删除[Author]: d

删除[Author]: s

删除[Author]: those

删除[Author]: provides

删除[Author]: has

删除[Author]: provide

删除[Author]: The h

删除[Author]: the abundance

删除[Author]: increases

suitable range being between 10 and 12 (Pierzynski et al., 1994). As Table 4 shows, N₂O emission was significantly related to the soil C:N ratios ($P < 0.05$), which means that denitrifying bacteria could use their endogenous carbon source for denitrification when the external carbon source was insufficient. Moreover, incomplete denitrification leads to the accumulation of NO₂-N, which is conducive to N₂O release. Meanwhile, due to the weak competitive ability of Nos to electrons, a low soil C:N ratio inhibits the synthesis of Nos, which is also a reason for N₂O release. In this study, all sites in transects T1–T4 exhibited similar soil C:N ratios in the optimum range (Table 1), which is favorable for microbial decomposition. However, the soil C:N ratios in transect T5 were higher than those in the other transects, especially in the dry lake bed. Therefore, transect T5 showed severe mineralization and a low microbial decomposition rate.

删除[Author]: that
删除[Author]: s
删除[Author]: are
删除[Author]: will
删除[Author]: is
删除[Author]: the
删除[Author]: the
删除[Author]:

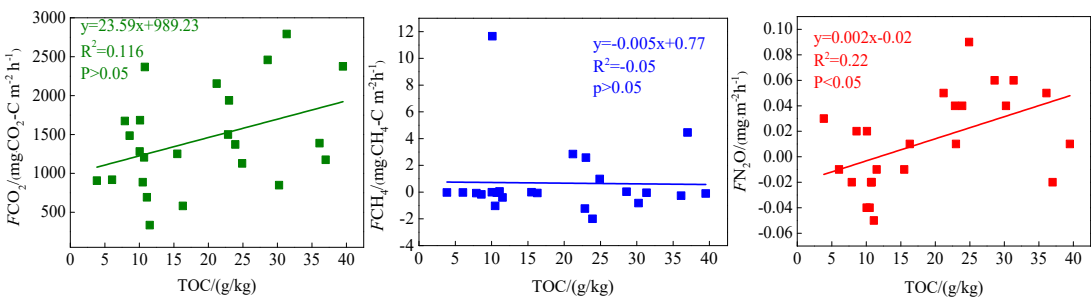


Fig. 8 Correlations between soil organic carbon (TOC) content and GHG emission (F)

删除[Author]: s

Table 4. Correlations between CO₂, CH₄, and N₂O emissions and impact factors ($n = 62$)

GHG flux	ST10	ST20	SMC10	SMC20	TOC	ρ_b	C:N	pH	EC	BIO
CO ₂	0.634**	0.592**	0.307*	0.216	0.393	-0.463**	-0.289*	-0.350**	-0.251*	0.491*
CH ₄	-0.029	-0.051	0.346**	0.353**	-0.02	-0.129	-0.156	-0.127	-0.107	0.607**
N ₂ O	0.127	0.118	0.304*	0.356**	0.493*	-0.194	0.311*	0.137	0.504**	0.251

Note: 1. The analysis method used in the table is Pearson correlation analysis, and the numbers represent Pearson correlation coefficients.

2. * and ** denote significant and highly significant correlations ($P < 0.01$ and $P < 0.05$), respectively.

3. ST - soil temperature, SMC - soil moisture content, ρ_b - soil bulk density, soil C:N - soil carbon-nitrogen ratio, pH - soil pH, EC - soil electrical conductivity, BIO - aboveground biomass

4.2 Riparian wetlands as hotspots of GHG emissions

489 The results of this study emphasized that the rate of CO₂ emission_v in the riparian wetlands
490 were higher than that in the hillslope grasslands_v owing to a variety of factors. ST is an important
491 factor affecting GHG emission_v. Mclain and Martens (2006) showed that seasonal fluctuations in
492 ST and SMC in semi-arid regions have important effects on CO₂, CH₄, and N₂O emissions in
493 riparian soils. Poblador et al. (2017) studied the GHG emission_v in forest riparian zones and
494 suggested that the difference in the CO₂ and N₂O emissions in these zones is caused by the spatial
495 gradient of the regional SMC. In this study, the upstream riparian wetlands were characterized by
496 higher TOC content, lower soil C:N ratio, and more abundant BIO than those in the hillslope
497 grasslands (Table 1). These soil conditions benefited the soil microbial activity, ultimately
498 enhancing respiration as well as CO₂ emissions. However, the CO₂ emission_v in the downstream
499 areas was nearly identical to that in the grasslands_v, likely because the wetlands gradually evolved
500 into grasslands after their degradation. N₂O emission_v showed spatial patterns similar to that of
501 CO₂ emission_v, likely because the CO₂ concentration_v was closely related to the nitrification and
502 denitrification processes. High CO₂ concentrations can promote the carbon and nitrogen cycles in
503 soil (Azam et al., 2005), increasing below ground C allocation, which is associated with increased
504 root biomass, root turnover, and root exudation. Elevated pCO₂ in plants, provides_v the energy for
505 denitrification in the presence of high available N, and there is increased O₂ consumption under
506 elevated pCO₂ (Baggs et al., 2003). Moreover, soil respiration increases during soil denitrification
507 (Liu et al., 2010; Christensen et al., 1990). In this study, a weak correlation was observed between
508 the CO₂ and CH₄ emissions in the riparian zones (r = 0.228), but CO₂ emission_v was significantly
509 correlated with N₂O emission_v (r = 0.322, P < 0.05). The soil became anaerobic in the riparian
510 areas as the SMC increased, and this was conducive to the survival of CH₄-producing bacteria and
511 to denitrification reactions, eventually leading to an increase in CH₄ and N₂O emissions. Jacinthe
512 et al. (2015) reported that inundated grassland-dominated riparian wetlands were CH₄ sinks (−1.08
513 ± 0.22 kg·CH₄-C ha^{−1}·yr^{−1}), and Lu et al. (2015) also indicated that grasslands were CH₄ sinks. In
514 our study, a marked water gradient across the transects led to the transformation of the soil from
515 anaerobic to aerobic soil, which changed the wetland to either a CH₄ source or sink. Therefore,
516 during the transition from the riparian wetlands to the hillslope grasslands, CH₄ sources only
517 appeared_v in the near-stream sites, while sinks appeared at other sites.
518 Further, we compared the GHG emissions in the riparian wetlands and the hillslope

删除[Author]: s
删除[Author]: those
删除[Author]: s
删除[Author]: s
删除[Author]: affected
删除[Author]: are
删除[Author]: s
删除[Author]: were
删除[Author]: those
删除[Author]: The
删除[Author]: s
删除[Author]: those
删除[Author]: the
删除[Author]: s
删除[Author]: s
删除[Author]: were
删除[Author]: in e
删除[Author]: Plants
删除[Author]: d
删除[Author]: or that
删除[Author]: was
设置格式[Author]: 字体: 非倾斜
删除[Author]: s
删除[Author]: were
删除[Author]: s
设置格式[Author]: 字体: 非倾斜
设置格式[Author]: 字体: 非倾斜
删除[Author]: function as
删除[Author]: emissions
删除[Author]: as sources
删除[Author]: and
删除[Author]: of

519 grasslands around the Xilin River Basin with those in various types of grasslands (meadow
520 grassland, typical grassland, and desert grassland) in the Xinlingol League in Inner Mongolia
521 (Table 5). CO₂ emission in the wet season decreased in the following order: upstream riparian
522 wetlands > downstream riparian wetlands > hillslope grasslands > meadow grassland > typical
523 grassland > desert grassland. Moreover, the upper riparian wetlands acted as source_s of CH₄
524 emission, while the downstream transects and grasslands served as CH₄ sinks. Similarly, except in
525 the downstream transects, N₂O emissions occurred as weak sources in different types of
526 grasslands and upstream riparian wetlands. The GHG emissions showed similar spatial patterns in
527 October. Although these estimates were made only in the growing season in August and the
528 non-growing season in October, our results suggest that the riparian wetlands are the potential
529 hotspots of GHG emission. Thus, it is important to study GHG emission to obtain a
530 comprehensive picture of the role of the riparian wetlands in climate change.

531

532 Table 5. GHG emission fluxes of riparian wetlands and grasslands

Sample plot	GHG emissions in August (mg·m ⁻² ·h ⁻¹)			GHG emissions in October (mg·m ⁻² ·h ⁻¹)			Reference
	CO ₂	CH ₄	N ₂ O	CO ₂	CH ₄	N ₂ O	
Wetlands of upstream transects (T1, T2, and T3)	n=13 1,606.28 ± 697.78	1.417 ± 3.41	0.031 ± 0.03	182.35 ± 88.26	0.272 ± 0.49	0.002 ± 0.005	This study
Wetlands of downstream transects (T4 and T5)	n=7 1,144.15 ± 666.50	-0.215 ± 0.45	-0.037 ± 0.05	98.13 ± 15.11	-0.015 ± 0.05	0.001 ± 0.01	
Hillslope grasslands of all transects	n=7 1,071.54 ± 225.39	-0.300 ± 0.40	0.003 ± 0.03	77.68 ± 25.32	-0.048 ± 0.03	-0.002 ± 0.005	
Meadow grassland	166.39 ± 45.89	-0.038 ± 0.009	0.002 ± 0.001	-	-	-	Guo et al., 2017
Typical grassland	240.32 ± 87.56	-0.042 ± 0.025	0.037 ± 0.034	-	-	-	
Desert grassland	107.59 ± 54.10	-0.036 ± 0.015	0.003 ± 0.001	-	-	-	
Typical grassland	520.25 ± 59.07	-0.102 ± 0.012	0.007 ± 0.001	88.34 ± 9.84	-0.099 ± 0.003	0.005 ± 0.001	Zhang, 2019
Typical grassland	232.42 ± 18.90	-0.090 ± 0.005	0.004 ± 0.001	-	-	-	Chao, 2019

Typical grassland	265.23 ± 31.43	-0.185 ± 0.018	0.005 ± 0.001	189.41 ± 28.96	-0.092 ± 0.012	0.004 ± 0.001
Meadow grassland	553.85	-0.163	0.003	47.73	-0.019	0.011
Geng, 2004						
Typical grassland	308.60	-0.105	0.002	70.25	-0.029	0.007

We roughly estimated the annual cumulative emission amounts of CO₂, CH₄, and N₂O from the riparian wetlands and hillslope grasslands around the Xilin River Basin, and further calculated their global warming potential. As Table 6 indicates, annual cumulative emissions of CO₂ and CH₄ decreased in the following order: upstream riparian wetlands > downstream riparian wetlands > hillslope grasslands, and N₂O in the following order: upstream riparian wetlands > hillslope grasslands > downstream riparian wetlands. In this study, we used the static dark-box method to measure CO₂ emissions, which does not consider the absorption and fixation of CO₂ by plant photosynthesis. Therefore, the total annual cumulative CO₂ emissions are high. This result clearly showed the more significant impact of CO₂ emission, than that of CH₄ and N₂O emissions on global warming. The GWP depends on the cumulative emissions of the GHGs. The GWPs shown in Table 6, were in the following order: upstream riparian wetlands (13,474.91 kg/hm²) > downstream riparian wetlands (8,974.12 kg/hm²) > hillslope grasslands (8,351.24 kg/hm²). Therefore, both the riparian wetlands and the grasslands are the “sources” of GHGs on a 100-year time scale. The source strength of the wetlands is higher than that of the grasslands, further indicating that the riparian wetlands are hotspots of GHG emission.

Table 6 Cumulative annual emission flux and global warming potential of GHGs in riparian wetlands and grasslands

Sample plot	CO ₂ /kg/hm ²	CH ₄ /kg/hm ²	N ₂ O/kg/hm ²	GWP/CO ₂ kg hm ²
Wetlands of upstream transects (T1, T2, and T3)	13,092.8±5378.16	12.36±26.40	0.25±0.23	13,474.91±5828.68
Wetlands of downstream transects (T4 and T5)	9,093.47±4831.82	-1.68±3.23	-0.26±0.40	8,974.12±4912.75
Hillslope grasslands of all transects	8,412.26±1614.26	-2.55±3.12	0.01±0.20	8,351.24±1648.22

删除[Author]: its
 删除[Author]: indicated
 删除[Author]: that
 删除[Author]: s'
 删除[Author]: that
 删除[Author]: s
 删除[Author]: is
 删除[Author]: as (
 删除[Author]:):
 删除[Author]: the
 删除[Author]: s

4.3 Effects of riparian wetland degradation on GHG emissions

The hydrology and soil properties showed evident differences between transects because the downstream zone was dry all year due to the presence of the Xilinhote Dam (Fig. 1). The dam caused the degradation of the riparian wetlands, resulting in reduced GHG emission. The average CO₂ emission, amounted to 1,663 mg·m⁻²·h⁻¹ in the upstream transects (T1, T2, and T3) at the riparian wetlands, while the downstream transects (T4 and T5) recorded an average emission of 1,084 mg·m⁻²·h⁻¹, 35% lower than that in the upstream transects. The N₂O emission, from the riparian wetlands was lower in the downstream transects.

Wetland degradation first resulted in the continuous reduction of SMC, which led to the deepening of the wetland's aerobic layer thickness. Besides, SMC may affect ST, and thus transport the CH₄ emissions from a source to a sink by affecting methanogen activity (Yan et al., 2018). Second, the reduction of SMC impeded physiological activities of aboveground plants, and inhabited related enzyme activities in the respiration process. Meanwhile, various enzyme reactions of underground microorganisms under water stress influence and reduced CO₂ emissions (Zhang et al., 2017). Finally, after wetland degradation, long-term drought led to an extremely low SMC, which is not conducive to the growth of nitrifying and denitrifying bacteria, and causes the transport of N₂O emissions from source to sink (Zhu et al., 2013). As Table 1 shows, soil TOC content in the upstream transects (average: 25.1 g·kg⁻¹) was higher than that in the downstream transects (average: 8.41 g·kg⁻¹). The relatively low SMC and the aerobic environment were conducive to the mineralization and decomposition of the TOC. The degradation of plants in the wetlands led to the gradual reduction of BIO. Ultimately, the plant carbon source input of the degraded wetlands decreased, and the bare land temperature increased due to the reduced plant shelter. This accelerated the decomposition of TOC, leading to its decrease. This result indicates that wetland degradation caused the soil carbon pool's loss and weakened the wetland carbon source/sink function. These results are in agreement with those of Xia (2017).

The degraded wetlands also caused soil desertification and salinization, leading to a decline in the physical protection afforded by organic carbon and a reduction in soil aggregates. Thus, the preservative effect, provided by organic carbon declined. The TOC content and SMC in the dry lake bed in transect T5 were relatively high; however, the GHG emission, was very low along this transect because soil pH values increased after the degradation of the lake soil, exceeding the

删除[Author]: among the
删除[Author]: s
删除[Author]: s
删除[Author]: in the riparian wetlands
删除[Author]: the value
删除[Author]: s
删除[Author]: were
删除[Author]:
删除[Author]: The w
删除[Author]: could
删除[Author]: 's change
删除[Author]: transformed
删除[Author]: s'
删除[Author]: ly
删除[Author]: s'
删除[Author]: physiological activities
删除[Author]: s'
删除[Author]: caused too
删除[Author]: was
删除[Author]: ,
删除[Author]: which caused
删除[Author]: transformation
删除[Author]: that
删除[Author]: is
删除[Author]: on
删除[Author]: ,
删除[Author]: but
删除[Author]: s
删除[Author]: were

optimum range required for microorganism activity. The soil C:N ratio was very high, resulting in severe mineralization and a low microbial decomposition rate, ~~thus affecting the~~ GHG emissions.

删除[Author]: hence

删除[Author]:

5. Conclusions

The riparian wetlands in the Xilin River Basin constitute a dynamic ecosystem. The present spatial and temporal transfers in the studied biogeochemical processes were attributed to the changes in SMC, ST, and soil substrate availability. Our simultaneous analysis of CO₂, CH₄, and N₂O emissions from ~~the~~ riparian wetlands and ~~the~~ hillslope grasslands in the Xilin River Basin revealed that the majority of the GHG emissions occurred in the form of CO₂. Moreover, our results clearly illustrate a marked seasonality and spatial pattern of GHG emissions along the transects and in the longitudinal direction (i.e., upstream and downstream). SMC and ST were two critical factors controlling the GHG emissions. Moreover, ~~the~~ abundant BIO promoted the CO₂, CH₄, and N₂O emissions.

删除[Author]: d

The riparian wetlands ~~are~~ potential hotspots of GHG emissions in the Inner Mongolian region. However, the degradation of ~~these~~ wetlands ~~has~~ transformed the area from a source to a sink for CH₄ and N₂O emissions, and ~~reduced~~ CO₂ emissions, which ~~has~~ severely affected the wetland carbon cycle processes. Our results show that ~~though~~ the riparian wetlands have high CO₂ emissions, ~~the~~ wetlands are CO₂ sinks, ~~due to the~~ photosynthesis of plants. Overall, our study suggests that anthropogenic activities have significantly changed the hydrological characteristics of the studied area, and ~~that this can~~ accelerate carbon loss from the riparian wetlands and further influence GHG emissions in the future.

删除[Author]: were the

删除[Author]: ,

删除[Author]:

删除[Author]: s

删除[Author]: but

删除[Author]: in the

删除[Author]: overall CO₂ balance general

删除[Author]: will

删除[Author]: the

Author Contributions

Xinyu Liu, Xixi Lu and Ruihong Yu designed the research framework and wrote the manuscript. Xixi Lu and Ruihong Yu supervised the study. Xinyu Liu, Hao Xue, Zhen Qi, Zhengxu Cao and Zhuangzhuang Zhang carried out the field experiments and laboratory analyses. Z.Z. drew ~~the~~ GIS mapping in this paper. Tingxi Liu proofread the manuscript. Heyang Sun contributed much ~~to~~ the revised version of our manuscript.

删除[Author]: experiments

删除[Author]: in

Acknowledgements

This study was funded by the National Key Research and Development Program of China (grant no. 2016YFC0500508), Major Science and Technology Projects of Inner Mongolia

Autonomous Region (grant nos. 2020ZD0009 and ZDZX2018054), National Natural Science Foundation of China (grant no. 51869014), Key Scientific and Technological Project of Inner Mongolia (grant no. 2019GG019), and Open Project Program of the Ministry of Education Key Laboratory of Ecology and Resources Use of the Mongolian Plateau (grant no. KF2020006).

Competing interests

The authors declare no conflicts of interest.

References

- Azam F., Gill S., Farooq S.: Availability of CO₂ as a factor affecting the rate of nitrification in soil, *Soil Biology & Biochemistry*, 37, 2141–2144, doi 10.1016/j.soilbio.2005.02.036, 2005.
- Baggs E.M., Richter M., Cadisch G., Hartwig U.A.: Denitrification in grass swards is increased under elevated atmospheric CO₂, *Soil Biology and Biochemistry*, 35, 729–732, doi 10.1016/S0038-0717(03)00083-X, 2003.
- Beger M., Grantham H.S., Pressey R.L., Wilson K.A., Peterson E.L., Dorfman D., Lourival R., Brumbaugh D.R., Possingham H.P.: Conservation planning for connectivity across marine, freshwater, and terrestrial realms, *Biological Conservation*, 143, 565–575, doi 10.1016/j.biocon.2009.11.006, 2010.
- Brady N C.: *Nature and properties of soils*, New Jersey: Prentice-Hall, Inc., doi 10.2307/3894608, 1999.
- Cao M., Yu G., Liu J., Li K.: Multi-scale observation and cross-scale mechanistic modelling on terrestrial ecosystem carbon cycle, *Science in China Ser. D Earth Sciences*, 48, 17–32, doi 10.1360/05zd0002, 2005.
- Chao R.: *Effects of Simulated Climate Change on Greenhouse Gas Fluxes in Typical Steppe Ecosystem*, Inner Mongolia University, 2019.
- Cheng S and Huang J.: Enhanced soil moisture drying in transitional regions under a warming climate, *Journal of Geophysical Research-Atmospheres*, 121, 2542–2555, doi 10.1002/2015JD024559, 2016.
- Christensen S., Simkins S., Tiedje J M.: Temporal Patterns of Soil Denitrification: Their Stability and Causes, *Soil Science Society of America Journal*, 54, 1614, doi 10.2136/sssaj1990.03615995005400060017x, 1990.

642 Ding W., Cai Z., Tsuruta H.: Cultivation, nitrogen fertilization, and set-aside effects on methane
643 uptake in a drained marsh soil in Northeast China, *Global Change Biology*, 10, 1801–1809, doi
644 10.1111/j.1365-2486.2004.00843.x, 2010. 删除[liuxinyu]: -

645 Enwall K., Philippot L., Hallin S.: Activity and composition of the denitrifying bacterial
646 community respond differently to long-term fertilization, *Applied and Environmental*
647 *Microbiology*, 71, 8335–8343, doi 10.1128/AEM.71.12.8335-8343.2005, 2005.

648 Fan X.: Research on nitrification potential and denitrification potential of soil in several farmland
649 in China, Nanjing Institute of Soil Sciences, Chinese Academy of Sciences, 1995.

650 Ferrón S., Ortega T., Gómez-Parra A., Forja J.M.: Seasonal study of dissolved CH₄, CO₂ and N₂O
651 in a shallow tidal system of the bay of Cádiz (SW Spain), *Journal of Marine Systems*, 66, 244–257,
652 doi 10.1016/j.jmarsys.2006.03.021, 2007.

653 Geng H.: Study on Charactors of CO₂, CH₄, N₂O Fluxes and the Relationship between Them and
654 Environmental Factors in the Temperate Typical Grassland Ecosystem, Northwest Agriculture &
655 Forestry University, 2004.

656 Gholz H.L., Wedin D.A., Smitherman S.M., Harmon M.E., Parton W.J.: Long-term dynamics of
657 pine and hardwood litter in contrasting environments: toward a global model of decomposition,
658 *Global Change Biology*, 6, 751–765, doi 10.1046/j.1365-2486.2000.00349.x, 2000.

659 Gou Q., Qu J., Wang G., Xiao J., Pang Y.: Progress of wetland researches in arid and
660 semi-ariregions in China, *Arid Zone Research*, 1001–4675, 213–220, 2015.

661 Guo X., Zhou D., Li Y.: Net Greenhouse Gas Emission and Its Influencing Factors in Inner
662 Mongolia Grassland, Chinese Grassland Society, 2017.

663 Heilman J.L., Cobos D.R., Heinsch F.A., Campbell C.S., McInnes K.J.: Tower-based conditional
664 sampling for measuring ecosystem-scale carbon dioxide exchange in coastal wetlands, *Estuaries*,
665 22, 584–591, doi 10.2307/1353046, 1999.

666 Inubushi K., Furukawa Y., Hadi A., Purnomo E., Tsuruta H.: Seasonal changes of CO₂, CH₄ and
667 N₂O fluxes in relation to land-use change in tropical peatlands located in coastal area of South
668 Kalimantan, *Chemosphere*, 52, 603–608, doi 10.1016/s0045-6535(03)00242-x, 2003.

669 IPCC.: Climate Change 2013: The Physical Science Basis. Contribution of Working, Working
670 Group I of the IPCC, 43, 866–871, 2013.

671 Jacinthe P.A., Vidon P., Fisher K., Liu X., Baker M.E.: Soil Methane and Carbon Dioxide Fluxes

672 from Cropland and Riparian Buffers in Different Hydrogeomorphic Settings, *Journal of*
673 *Environment Quality*, 44, 1080–1115, doi 10.2134/jeq2015.01.0014, 2015.

674 Johnson-Randall L.A., Foote A.L.: Effects of managed impoundments and herbivory on wetland
675 plant production and stand structure, *Wetlands*, 25, 38–50, doi
676 10.1672/0277-5212(2005)025[0038:eomiah]2.0.co;2, 2005.

677 Koops J.G., Oenema O., Beusichem M.L.: Denitrification in the top and sub soil of grassland on
678 peat soils, *Plant and Soil*, 184, 1–10, doi 10.1007/bf00029269, 1996.

679 Kou X.: Study on Soil Physicochemical Properties and Bacterial Community Characteristics of
680 River Riparian Wetland in Inner Mongolia Grassland, Inner Mongolia University, 2018.

681 Liu C.: Effects of Nitrogen Addition on the CO₂ Emissions in the Reed (*Phragmites australis*)
682 Wetland of the Yellow River Delta, China, Liaocheng University, 2019.

683 Liu C., Xie G., Huang H.: Shrinking and drying up of Baiyangdian Lake wetland: a natural or
684 human cause? *Chinese Geographical Science*, 16, 314–319, 2006.

685 Liu F., Liu C., Wang S., Zhu Z.: Correlations among CO₂, CH₄, and N₂O concentrations in soil
686 profiles in central Guizhou Karst area, *Chinese Journal of Ecology*, 29, 717–723, doi
687 10.1016/S1872-5813(11)60001-7, 2010.

688 Liu J., Wang J., Li Z., Yu J., Zhang X., Wang C., Wang Y.: N₂O Concentration and Its Emission
689 Characteristics in Sanjiang Plain Wetland, *Chinese Journal of Environmental Science*, 24, 33–39,
690 2003.

691 Lu Y., Song C., Wang Y., Zhao Z.: Influence of plants on CO₂ and CH₄ emission in wetland
692 ecosystem, *Acta Botanica Boreali-Occidentalia Sinica*, 27, 2306–2313, 2007.

693 Lu Z., Du R., Du P., Li Z., Liang Z., Wang Y., Qin S., Zhong L.: Effect of mowing on N₂O and
694 CH₄ fluxes emissions from the meadow-steppe grasslands of Inner Mongolia, *Frontiers of Earth*
695 *Science*, 9, 473–486, doi 10.1007/s11707-014-0486-z, 2015.

696 Lv M., Sheng L., Zhang L.: A review on carbon fluxes for typical wetlands in different climates of
697 China, *Wetland Science*, 11, 114–120, doi CNKI:SUN:KXSD.0.2013-01-020, 2013.

698 Malhl S.S., McGill W.B.: Nitrification in three Alberta soils: effects of temperature, moisture and
699 substrates concentration, *Soil Biology and Biochemistry*, 14, 393–399, doi
700 10.1016/0038-0717(82)90011-6, 1982.

701 McInain J E T., Martens D.A.: Moisture controls on trace gas fluxes in semiarid riparian soils, *Soil*

删除[liuxinyu]:

702 Science Society of America Journal, 70, 367, doi 10.2136/sssaj2005.0105, 2006.

703 Meng W., Wu D., Wang Z.: Control factors and critical conditions between carbon sinking and
704 sourcing of wetland ecosystem, Ecology and Environmental Sciences, 20, 1359–1366, doi
705 10.1016/S1671-2927(11)60313-1, 2011.

706 Mitsch W.J., Gosselink J.G.: Wetlands (Fourth Edition), John Wiley & Sons Inc.: Hoboken, New
707 Jersey, USA, 2007.

708 Mitsch W.J., Gosselink J.G., Anderson C.J., Anderson, C. J.: Wetland ecosystems: John Wiley &
709 Sons, 2009.

710 Moldrup P., Olesen T., Schjønning P., Yamaguchi T., Rolston D.E.: Predicting the gas diffusion
711 coefficient in undisturbed soil from soil water characteristics, Soil Science Society of America
712 Journal, 64, 1588–1594, doi 10.2136/sssaj2000.64194x, 2000.

713 Morley N., Baggs E.M.: Carbon and oxygen controls on N₂O and N₂ production during nitrate
714 reduction, Soil Biology & Biochemistry, 42, 1864-1871, doi 10.1016/j.soilbio.2010.07.008, 2010.

715 Naiman R.J., Decamps H.: The ecology of interfaces: Riparian zones, Annual Review of Ecology
716 & Systematics, 28, 621–658, doi 10.2307/2952507, 1997.

717 National Agricultural Technology Extension Service Center (NATESC): Technical specification
718 for soil analysis, 2006.

719 Niu C., Wang S., Guo Y., Liu W., Zhang J.: Studies on variation characteristics of soil nitrogen
720 forms, nitrous oxide emission and nitrogen storage of the Phragmites australis-dominated
721 land/inland water ecotones in Baiyangdian wetland, Journal of Agricultural University of Hebei,
722 40, 72–79, 2017.

723 Pierzynski G M S., J.T., Vance, G.F.: Soils and Environmental Quality, 1994.

724 Poblador S., Lupon A., Sabaté S., Sabater F.: Soil water content drives spatiotemporal patterns of
725 CO₂ and N₂O emissions from a Mediterranean riparian forest soil, Biogeosciences Discussions, 14,
726 1–28, doi 10.5194/bg-14-4195-2017, 2017.

727 Qin S., Tang J., Pu J., Xu Y., Dong P., Jiao L., Guo J.: Fluxes and influencing factors of CO₂ and
728 CH₄ in Hangzhou Xixi Wetland, China, Earth and Environment, 44, 513–519, 2016.

729 Sjögersten S., Wal R V.D., Woodin S.J.: Small-scale hydrological variation determines landscape
730 CO₂ fluxes in the high Arctic, Biogeochemistry, 80, 205–216, doi 10.2307/20456398, 2006.

731 Sun Y., Wu H., Wang Y.: The influence factors on N₂O emissions from nitrification and

denitrification reaction, *Ecology and Environmental Sciences*, 20, 384–388, doi
10.1631/jzus.B1000275, 2011.

Tong C., Wu J., Yong S., Yang J., Yong W.: A landscape-scale assessment of steppe degradation in
the Xilin River Basin, Inner Mongolia, China, *Journal of Arid Environments*, 59, 133–149, doi
10.1016/j.jaridenv.2004.01.004, 2004.

Ulrike R., Jürgen A., Rolf R., Wolfgang M.: Nitrate removal from drained and reflooded fen soils
affected by soil N transformation processes and plant uptake, *Soil Biology and Biochemistry*, 36,
77-90, doi 10.1016/j.soilbio.2003.08.021, 2004.

Waddington J.M., Roulet N.T.: Carbon balance of a boreal patterned peatland, *Global Change
Biology*, 6, 87–97, doi 10.1046/j.1365-2486.2000.00283.x, 2000.

Whiting G.J., Chanton J.P.: Greenhouse carbon balance of wetlands: methane emission versus
carbon sequestration, *Tellus B*, 53, 521-528, doi 10.3402/tellusb.v53i5.16628, 2001.

WMO.: WMO Statement on the State of the Global Climate in 2017, World Meteorological
Organization, 2018.

Xi X., Zhu Z., Hao X.: Spatial variability of soil organic carbon in Xilin River Basin, *Research of
Soil and Water Conservation*, 24, 97–104, 2017.

Xia P., Yu L., Kou Y., Deng H., Liu J.: Distribution characteristics of soil organic carbon and its
relationship with enzyme activity in the Caohai wetland of the Guizhou Plateau, *Acta Scientiae
Circumstantial*, 37, 1479–1485, doi 10.13671/j.hjkxxb.2016.0129, 2017.

Xu H., Cai Z., Yagi K.: Methane Production Potentials of Rice Paddy Soils and Its Affecting
Factors, *Acta Pedologica Sinica*, 45, 98–104, doi 10.1163/156939308783122788, 2008.

Yan L., Zhang X., Wang J., Li Y., Wu H., Kang X.: Drainage effects on carbon flux and carbon
storage in swamps, marshes, and peatlands, *Chin J Appl Environ Biol*, 24, 1023–1031, doi
10.19675/j.cnki.1006-687x.2017.11031, 2018.

Yu P., Zhang J., Lin C.: Progress of influence factors on N₂O emission in farmland soil,
Environment and sustainable development, 20–22, 2006.

Zhang D.: Effects of Different Grazing Intensities on Greenhouse Gases Flux in Typical Steppe of
Inner Mongolia, Inner Mongolia University, 2019.

删除[liuxinyu]: ;

760 Zhang Y., Hao Y., Cui L., Li W., Zhang X., Zhang M., Li L., Yang S., Kang X.: Effects of extreme
761 drought on CO₂ fluxes of Zoige alpine peatland, Journal of University of Chinese Academy of
762 Sciences, 34, 462-470, 2017.

763 Zhang Z., Hua L., Yin X., Hua L., Gao J.: Nitrous oxide emission from agricultural soil land some
764 influence factors, Journal of Capital Normal University: Natural Science Edition, 26, 114–120,
765 2005.

766 Zhu X., Song C., Guo Y., Shi F., Wang L.: N₂O emissions and its controlling factors from the
767 peatlands in the Sanjiang Plain, China Environmental Sciences, 33, 2228–2234, 2013.

768 Zona D., Oechel W.C., Kochendorfer J., Paw U K.T., Salyuk A.N., Olivas P.C., Oberbauer S.F.,
769 Lipson D.A.: Methane fluxes during the initiation of a large-scale water table manipulation
770 experiment in the Alaskan Arctic tundra, Global Biogeochem Cycles, 23, doi
771 10.1029/2009gb003487, 2009.

删除[liuxinyu]: -